International Journal of the Physical Sciences Vol. 6(13), pp. 3218–3231, 4 July, 2011
Available online at http://www.academicjournals.org/IJPS
DOI: 10.5897/IJPS10.466
ISSN 1992 - 1950 ©2011 Academic Journals

Full Length Research Paper

Exit-selection behaviors during a classroom evacuation

Lim Eng Aik

Institute Matematik Kejuruteraan, Universiti Malaysia Perlis, Perlis, Malaysia. E-mail: e.a.lim80@gmail.com
Tel: 6049855485.

Accepted 25 March, 2011

A modified version of the existing Cellular Automata (CA) model is proposed to simulate an evacuation experiment conducted in a classroom with and without obstacles. This work present the use of CA with neural network decision-making capabilities to simulate an exit-selection phenomenon in the experiment, and an intelligent exit-selection behavior was observed in our model. The experimental and simulation results are reasonable, while our simulation results agree with the experimental results quite closely. From the simulation results it is observed that occupants tend to select the exit closest to them when the density there is low, but if the density is high, they will go to an alternative exit so as to avoid a long wait. This reflects the fact that occupants may not fully utilize multiple exits during evacuation. The improvement of our proposed model is valuable for further study and for upgrading the safety aspects of building design.

Key words: Cellular automata, probabilistic neural network, floor-field model, output flux, intelligent agent.

INTRODUCTION

Pedestrian evacuation is a multi-agent system comprised of local interactions between people and the environment (e.g. walls) which determine people's global behaviors, e.g., clogging and 'faster-is-slower' phenomena (Helbing et al., 2000; Helbing and Molnar, 1995; Song et al., 2006). Kirchner et al. (2003) introduced the floor field model in a cellular automaton (CA) system to quantify the desired walking direction (Burstedde et al., 2001) of occupants. The model calculates the floor field values corresponding with the influences of building geometry and occupant movement, and generates numerous characteristics of occupant dynamics, mainly in distinctive group effects. The concept of floor field has been used in many evacuation models (Alexandre and Bastien, 2003; Zhao et al., 2008; Yang et al., 2005; Zhao et al., 2006; Varas et al., 2007; Pablo et al., 2007; Fang et al., 2010; Liu et al., 2009).

A discrete model such as the CA model quantifies the evacuation area with discrete lattice cells (Song et al., 2006). Each cell can be either empty or occupied by an occupant or an obstacle. An occupant can only move to an empty neighboring cell in each time-step. Further study of the evacuation process and the affect of discretization on occupant dynamics using a multi-grid model was carried out by Song et al. (2006), who found that the evacuation time is associated with the grid size and the length of the time-step (Xu et al., 2008). Recently, a multi-floor field CA was reported (Peng and Chou, 2011). Many researchers mainly focus on smoothing the movement of CA model in an open area, for example, introducing a learning algorithm into CA for movement near corner turning area (Ishii and Morishita, 2010), and some of them defined a cost function as precondition in CA agent movement to improved agents collision and congestion avoidance capability (Wang et al., 2010). But none of above works is mainly focus on exit selection in a confined room with multiple exits. Varas and his colleague simplify the Kirchner floor-field model (Kirchner et al., 2003) by investigating the same crowd flow going out of a hall with a CA model (Varas et al., 2007). However, this model has limited intelligence in selecting an exit during evacuation. The model is helpful in simulating collective phenomena such as jams, blocks, and clogging, but is not good at describing intelligent exit-selecting behaviors in evacuations.

In this paper, we proposed an intelligent CA model that capable of reproduced realistic behaviors of occupants leaving a room. We reconstruct a classic CA model from (Varas et al., 2007) then we incorporate neural network as its decision-making system. The Probabilistic Neural Network (PNN) is selected based on its excellent classification and fast training abilities as reported in (Muniz et al., 2010; Mckenzie et al., 2010; Wang et al., 2009) compared to other slow training neural network

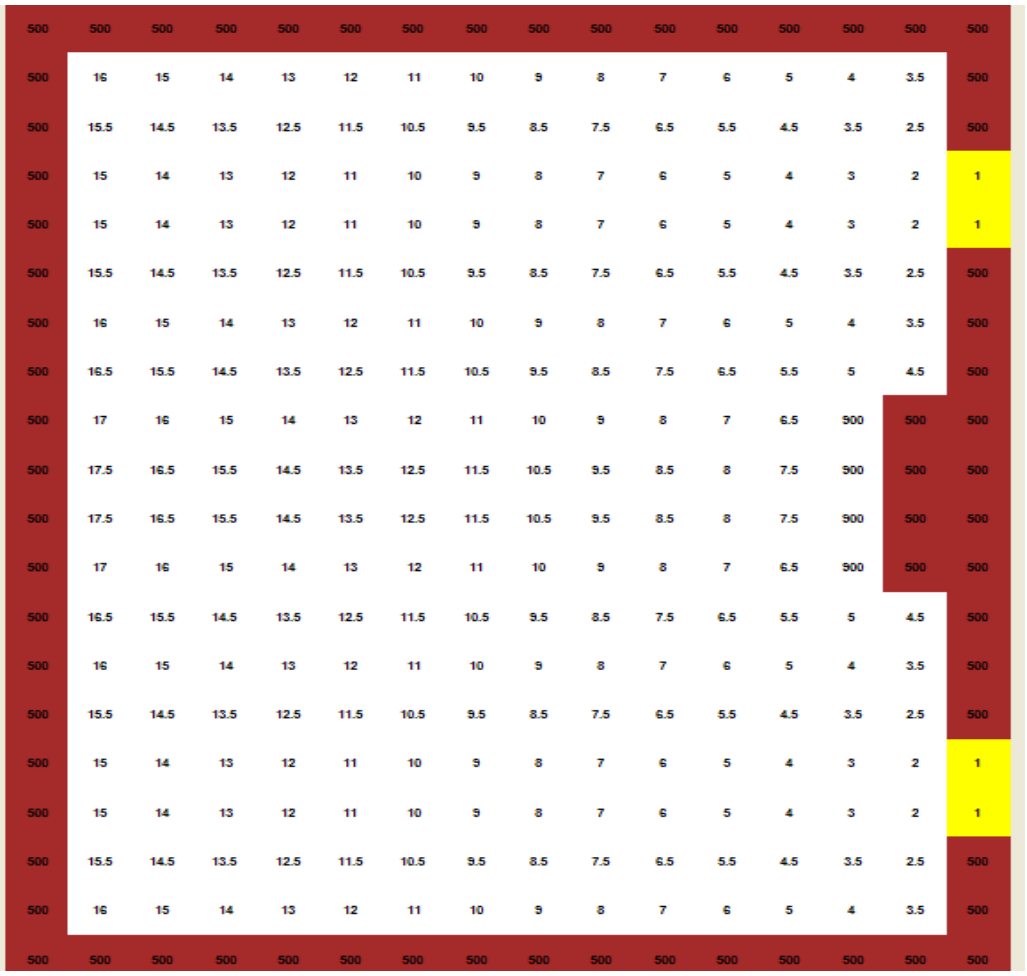

Figure 1. Floor weighting for a room with a 20 x 16 grid.

model, e.g. Backpropagation network and Radial Basis Function network. The logic is that a fast trained model is able to smooth the whole evacuation simulation process by reducing the decision-making time. The results from the simulations of the evacuation process (e.g. occupant exit selecting intelligence as well as the evacuation time) are then compared with the classic CA model and real-world experiment results.

MODEL DESCRIPTION

The room is represented by a two-dimensional grid. Each cell in the grid can be either empty or occupied by an obstacle or one occupant. The size of a cell is 0.5 x 0.5 m^2, the typical space occupied by a single occupant in a dense situation (Teknomo and Millonig, 2007). Considering that the mean velocity of an occupant is 1.0 m/s (Burstedde et al., 2001; Zhao et al., 2006; Helbing et al., 2003), moving 0.5 m per time-step Δt yields $\Delta t = 0.5$ s.

Floor field

Consider a room with fixed dimensions. Each cell is assigned with a value representing its weight value to the exit with a principle such that occupant will always travel to a cell with a lower value than their current one. Lower weights correspond to cells nearer the exit. In short, the floor field is formed by a rectangular grid with weight for each exit is assigned as 1, while its adjacent cells value are assigned according to the rules defined by [11] as follows:

If a cell is assigned a value M, adjacent cells in the vertical or horizontal directions are each assigned a value M + 1. For diagonal directions, a value of M + λ is assigned adjacent cells, where $\lambda = 1.5$.

The weight assigning process is repeated until all cells are evaluated and each wall in the field is also considered in weighting by giving a very high weighted value to ensure occupants will never occupy them. Figure 1

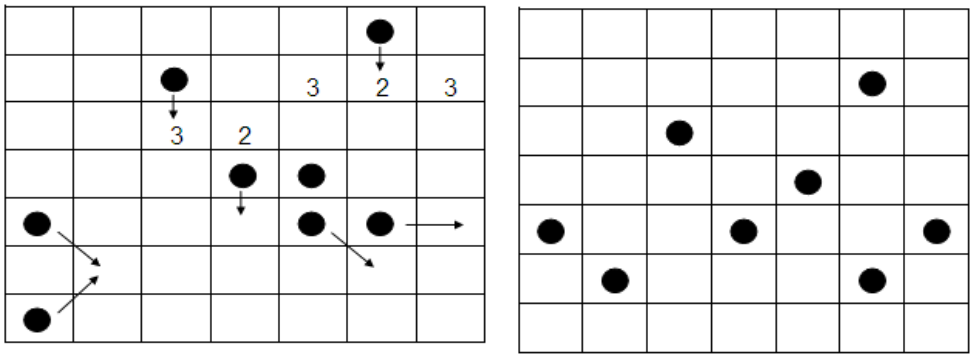

Figure 2. Possible movement for occupants in this CA model.

shows the floor weightings obtained by these rules in a 20 x 16 grid room with two exits in the right wall.

Occupant movement and interaction

At each iteration, occupants must decide where to move. To make this model non-deterministic, a set of intelligent local rules are introduced (Zhao et al., 2006):

(1) Determine the weighted value of each cell based on the distance between the exits, the location of the walls, and the distribution of occupants. The closer to exits, the lower the weight;
(2) Each occupant chooses one of the neighboring cells based on their weighting in the grid;
(3) If multiple occupants try to enter the same cell, they are assigned a random number and the occupant with the highest value moves there.

To preclude a deterministic model, an occupant is allowed to move to a higher weighted unoccupied cell when the lower-weighted neighboring cell is too crowded. This movement is decided by neural network decision making, described in Section 3. These features are summarized in Figure 2.

USE OF NEURAL NETWORK FOR EXIT SELECTION

General description of Probabilistic Neural Network (PNN)

PNN is an excellent classifier that based on Bayesian decision-making and nonparametric techniques on estimate Probability Density Function (PDF) in the form of a Gaussian distribution (Specht, 1990) as show in the Equation (1). We applied PNN to classify the location of neighboring cell that suitable to move-in next, based on the training data and information from the surrounding of that particular occupant as discuss in the next section.

$$f_i(X) = \left(\frac{1}{N_i}\right)\left(\frac{1}{(2\pi)^{m/2}}\right)\left(\frac{1}{\sigma^m}\right)\sum_{j=1}^{N_i}\exp\left(-\frac{\|X_i - X_j\|^2}{2\sigma^2}\right) \quad (1)$$

Since PNN is applicable to general classification problems, and assumes that the eigenvector to be classified must belong to one of the known classifications, the absolute probabilistic value of each classification is not important and only relative values need to be considered, hence, in Equation (1),

$$\left(\frac{1}{(2\pi)^{m/2}}\right)\left(\frac{1}{\sigma^m}\right)$$

can be ignored and Eq. (1) can be simplified as

$$f_i(X) = \left(\frac{1}{N_i}\right)\sum_{j=1}^{N_i}\exp\left(-\frac{\|X_i - X_j\|^2}{2\sigma^2}\right) \quad (2)$$

In equation (2), σ is the smoothing parameter of PNN. After network training is completed, prediction accuracy can be enhanced through the adjustment of the smoothing parameter σ; that is the larger the value, the smoother the approaching function. If the smoothing parameter σ is inappropriately selected, it will lead to excessive or insufficient neural units in the network design, and over fitting or inappropriate fitting will be the result in the function approximation attempt; predictive power will be also be reduced. Let:

$$d_{ij} = \|X_i - X_j\|^2$$

be the cell of the Euclidean distance of two points X_i and X_j in the sample space, then, Equation (2) can be re-written as:

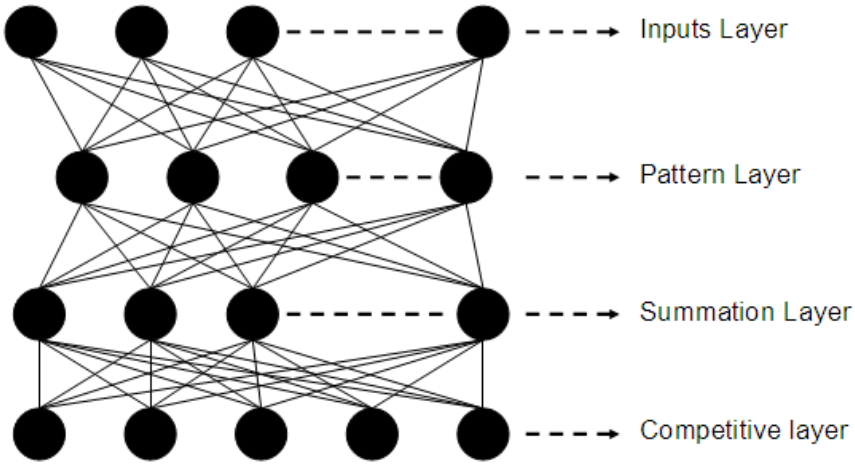

Figure 3. Architecture of the PNN.

$$f_i(X) = \left(\frac{1}{N_i}\right)\sum_{j=1}^{N_i}\exp\left(-\frac{d_{ij}}{2\sigma^2}\right) \quad (3)$$

In Equation (3), when the smoothing parameter σ approaches zero,

$$f_i(X) = \frac{1}{N_i}$$

If $X_i = X_j$, then

$$f_i(X) = 0$$

At this moment, PNN will depend fully on the non-classified closest to the classified sample to decide its classification. When the smoothing parameter σ approaches infinity,

$$f_i(X) = 1$$

PNN is a four-layer feed-forward neural network. Each level is directly connected with all neurons of the following level but there is no connection with the neurons of the same layer. A typical architecture is shown below in Figure 3. The first layer is the input layer and the number of neural units is the number of independent variables which handle the input data; the second layer is the pattern layer, which stores the training data; the data sent out by the pattern layer will pass through the neural unit of the third layer, the summation layer, where the calculation of the Equation (3) is performed. The fourth layer is the competitive layer and its competitive transfer function will pick up, from the output of the last layer, the maximum value from these probabilities and generate the output value. If the output value is 1, it means it is the category you want; but if the output value is 0, it means it is the other unwanted category.

The training for exit-selection

In this section, we explained the use of PNN as the intelligent controller navigating occupants to the least busy exit. The input matrix for PNN is set to *m* x *n* dimensions, where *n* is the number of variables selected for training the network and *m* is the number of training data sets. There are 8 variables selected from the clusters identified by the cellular automaton:

Left (*L*) = left cell of occupant neighborhood
Left-front (*LF*) = left-front cell of occupant neighborhood
Front (*F*) = front cell of occupant neighborhood
Right-front (*RF*) = right-front cell of occupant neighborhood
Right (*R*) = right cell of occupant neighborhood
Distance to alternative exit: If distance to the nearest exit, $k < d$, where *d* is the threshold value for distance, then value 0 is assigned to the matrix array, otherwise value 1 is assigned.
Occupant neighborhood movement status: if static (value = 0) or moving (value = 1).
Direction of alternate exit: right (*ur*), front (*uf*), and left (*ul*).

The cells are given the value 1 if the subspace for the obstacle position: *L*, *LF*, *F*, *RF*, and *R*, have obstacles, otherwise the value 0 is given. Ultimately, the direction of alternative exits for right, front and left are each assigned the values 1, 2, and 3 respectively. The 8 variables are

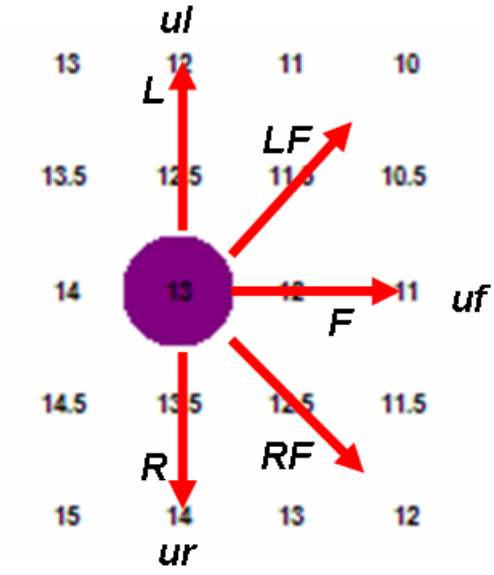

Figure 4. Occupant walk-space and subspaces.

used as inputs and the output consists of 5 variables. Network training was performed using 384 input-output data pairs from all possible movement within the cells neighborhood. The learning step for this network was completed after 250 iterations. When the CA simulation was begun, each moving step of the occupants was fed to the PNN, and feedback from the networks gave the decision to either go towards the alternative exit, or towards the alternate nearest exit. Figure 4 shows how the occupant walk-space can be divided into subspaces explained above. The algorithm of PNN decision-making is shown in Figures 5 and 6 shows its overall structure.

EXPERIMENT

The experiment was conducted in a 9.0 m x 14.0 m classroom (Figure 1); Figure 7 shows snapshots of the evacuation experiment from a camera. There are two 0.6 m wide exits in the classroom. For simulation purposes, the classroom is divided into an 18 x 14 grid of 0.5 m x 0.5 m cells. 50 students aged between 21 to 23 years took part in the experiment. The evacuation process was recorded by a camera in the corner of the classroom.

Two scenarios are designed in this experiment. The experiment is conducted only one time. Even though results from a single experiment may be unstable, they still reflect people's realistic performance and are adequate for use in this paper.

For Experiment 1, 50 people are randomly placed at the corner of lower wall in the classroom. The room is clear of obstacles and all exits are open. Experiment 2 is the same except for some obstacles in the middle of the room. In our experiment, all students are standing and are ready to evacuate at an audio signal. Pre-movement time (Helbing et al., 2000) where students tidy-up their property before evacuating the room can be ignored here.

The numbers of evacuees versus evacuation time in the two experiments are shown in Figure 11. We observed that the total evacuees versus evacuation time increases when the students as occupants utilize all the exits. In Experiment 2, with obstacles in the room, the evacuation time increased. This means that in process of evacuating the room with obstacles, besides the spatial distance to the exits, occupants' evacuation time is also determined by the path they choose to exit. The experimental data are shown in Table 1.

In Experiments 1 and 2, we clearly see clogging at an exit, and some students utilize an alternate exit. This means that student evacuation behavior is influenced by occupant densities around the exits. Accordingly, we modified an existing CA model to improve its intelligence in exit-selection and to simulate this dynamic process.

RESULTS AND DISCUSSION

Simulation results: room without obstacles

In Simulations 1 and 2, the room is divided into an 18 x 14 grid of 0.5 x 0.5 m cells (Fig. 1). There are 50 occupants in this simulation and the area of the room is 62 m^2, so the average density of occupants is 0.81 occupants/m^2. We set the time-step in the model as 0.5s based on Varas et al. (2007), and to guarantee the reliability of the results every simulation result mentioned in this paper is based on an average value of 10 times runs. In Simulation 1, the simulation was run based on the model proposed by Varas et al. (2007), while Simulation 2 was run using the new model proposed in this paper.

The whole evacuation lasted 17 and 14 s for Simulations 1 and 2 respectively. This obviously showed that the proposed evacuation model can save 3s compared to the Varas model (Table 1). We observed that the velocity of the occupants in the initial 3s is generally higher in both simulations. This is due to the lower density at the exit which makes a smooth occupant flow in the initial 3 s (Figures 11 (a), (b), (c)) as occupants evacuate at their desired velocity of about 1.0 m/s.

From Table 1, it can be seen that in Simulation 1, there is a different average evacuation velocity: 23% lower compared to Simulation 2. Due to the nature of the model proposed in (Varas et al., 2007) based on floor-field weights to select the nearest exit, this results in an overflow of occupants at the lower exit compared to the upper exit in Simulation 1. Density at the lower exit started to grow after the initial 3s and remained high for the next 10 s before falling linearly. In Simulation 2, the lower exit was only crowded for 6 s and the upper exit for only 2 s (Figure 8 (a), (b), (c)). The occupants were distributed at two exits rather than just the single exit as in Simulation 1.

Figure 9 (a), (b) and (c) shows the occupant flow rate to each exit against time. It is found that the flow rate through the lower exit in Simulation 1 was higher than the upper exit which is 0. Similar results were observed in Simulation 2 where the flow rate to the lower exit was also still higher than the upper exit. Fang et al. (2010) showed that occupants select the closest exit when there is no serious obstacle in front of them, even though another exit may be only a little further away, but when an obstacle

```
Procedure of exit selection
Begin
P_ij = occupant i with j-th variable
C_ij = floor-field weight for occupant i-th upper 5 cells, j = 1,2,…5
Occupant start to move according to floor weight

While not (cycle end)
    If obstacle around
        P_ij = 1 for obstacle cell found in neighbouring cells (j = 1,2,..,5),
        P_ij = 0 if the cell empty
        If alternative exit exist
            Occupant distance to alternative exit
            If distance > d
                P_ij = 1 for j = 6.
                If neighbouring cells static
                    P_ij = 1 for j = 7
                    Check direction of alternative exit:
                    U_i = max(C_ij)
                    P_ij = n for j = 8
                    where n = 1 (ur), 2 (uf), and 3 (ul)
                Else
                    P_ij = 0 for j = 7
            Else
                P_ij = 0 for j = 6
        Else
            Goto floor-field
    Else
        floor-field
End While
```

Figure 5. The algorithm for input data of PNN decision-making.

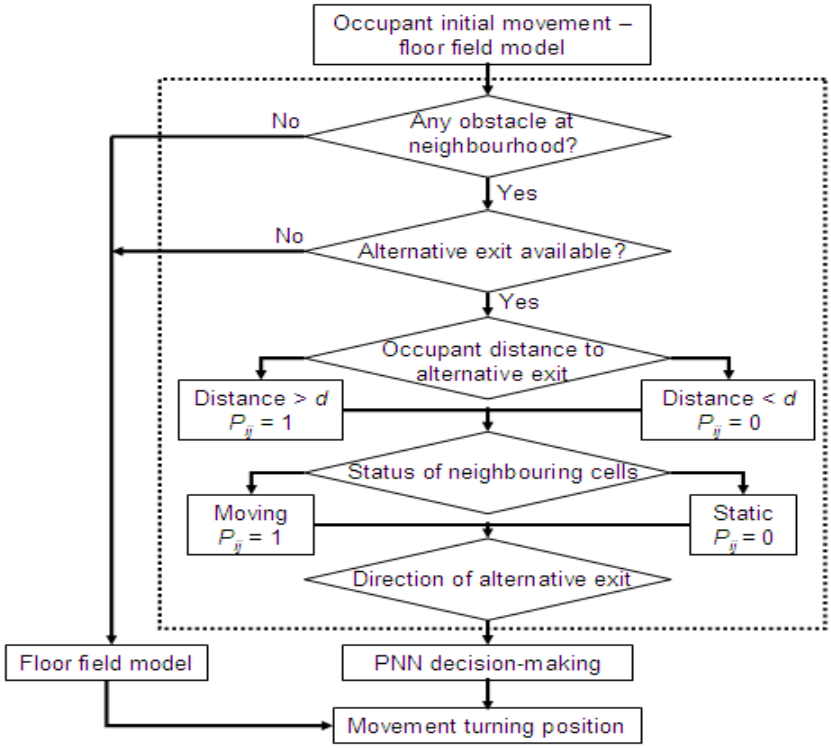

Figure 6. The structure of PNN decision-making.

(a) (b)

Figure 7. Snapshots of the evacuation experiment from camera.

Table 1. Simulation and experiment results.

	Rate of choosing upper exit, C_{upper} (%)	Total evacuation time (s)	Average evacuation time (s)	Average evacuation velocity (m/s)
Experiment 1	28.00	12.18	7.61	0.75
Simulation 1	0.00	17.00	9.55	0.56
Simulation 2	22.00	14.00	8.55	0.69
Experiment 2	46.00	15.30	10.88	0.84
Simulation 3	100.00	31.00	17.27	0.41
Simulation 4	52.00	18.00	12.40	0.77

obstacle appears and the occupants cannot move to the target exit at their desired velocity, they will try to find an alternative exit. This behavior can only be observed in our proposed model in Simulation 2. It can be seen from Figure 10 (a) and (b) that the curves representing the total occupants evacuating the room differ between Simulations 1 and 2. The difference between Simulations 1 and 2 gradually increases after 3 s. When the time reaches 11 s, this difference reaches a maximum, and the total number of occupants evacuating the room in Simulation 2 exceeds Simulation 1 by about 31%.

Simulation results: room with obstacles

For Simulations 3 and 4, we consider a room with an 18 x 14 grid of 0.5m x 0.5m cells, but with obstacles in it. There was a total 50 occupants for both the simulations. The area of the room currently is 58.75 m^2, so the average density of occupants in both Simulations 3 and 4 is 0.85 occupants/m^2. We used the same time-step and term in obtaining simulation results as in Simulations 1 and 2. Here, our proposed model simulation was utilized in Simulation 4. After both simulations were done, comparisons for more intelligent occupants in both models could be made.

Based on Table 1, we observed that the whole evacuation time was reduced by about 42% for Simulation 4 compared to Simulation 3. This is due to the behavior shown by Fang et al. (2010) that, in a real-world situation, when a blockage appears at an occupant's nearest target exit and they are not able to move at their desired velocity, they will move to an alternative exit. The individual occupant evacuation time also fell approximately 28% for Simulation 4 in contrast to Simulation 3.

From Figure 11 (d) and (e), we see that the velocity of the occupants in the initial 5 s is higher than that at other times in Simulation 3. Due to the lower density at the exits for the first 5 s, the occupant flow is smooth and moving at the desired velocity of 1.0 m/s. In Simulation 4, during the first 5 s, the same behavior occurs as in Simulation 3, but in the last 3 s, most of the occupants have already evacuated the room, so the room density gradually falls and the occupants are now able to move at their desired velocity.

As observed in Table 1, there is an 87% (higher) difference in average evacuation velocity in simulation 3. The cause of this can be observed in Figure 12: the blockage near the upper exit in Simulation 3 reduced the

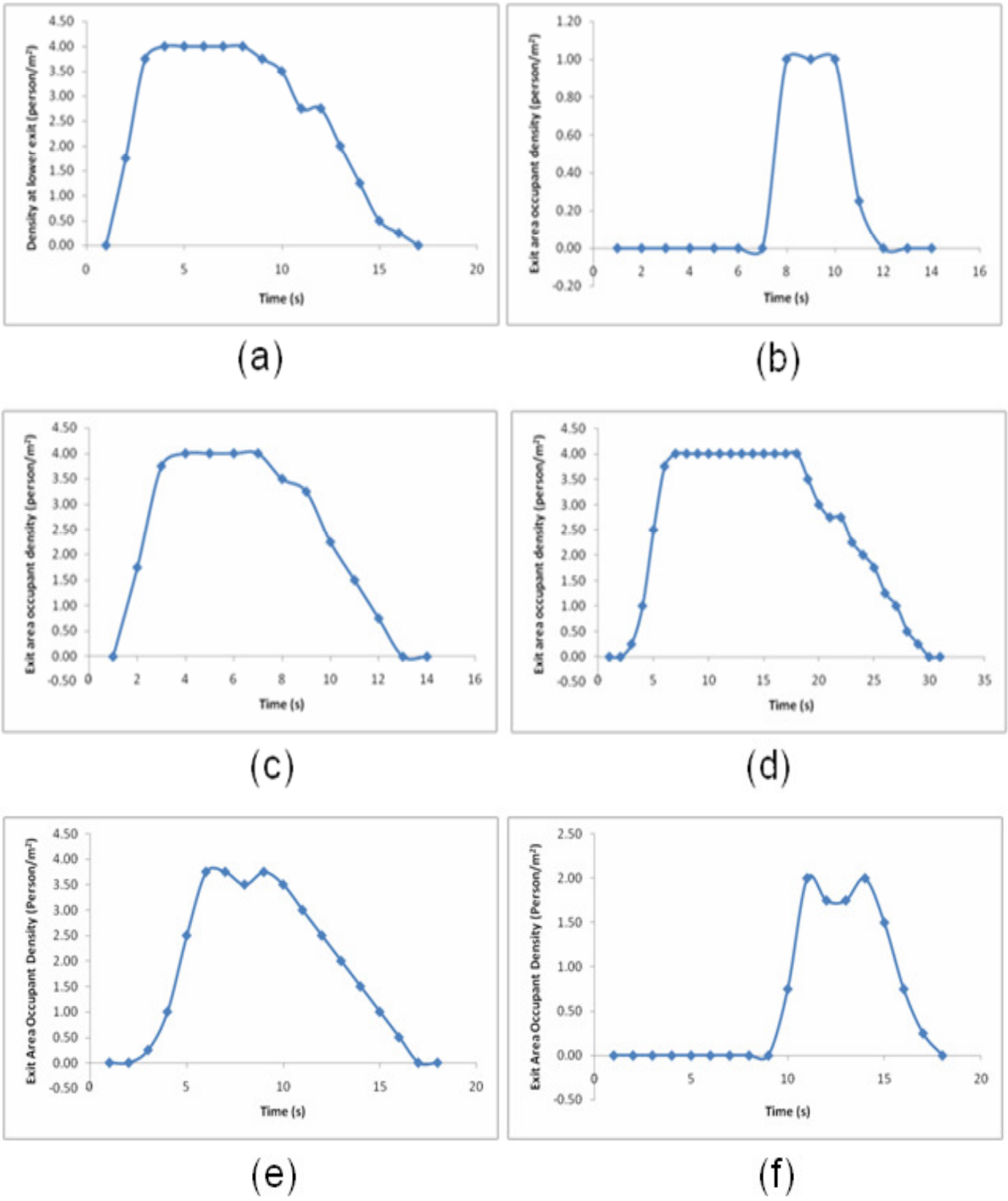

Figure 8. Plot for density at exit vs. time. Plot (a) for simulation 1, (b) and (c) for simulation 2, while (d) for simulation 3, lastly (e) and (f) are for simulation 4.

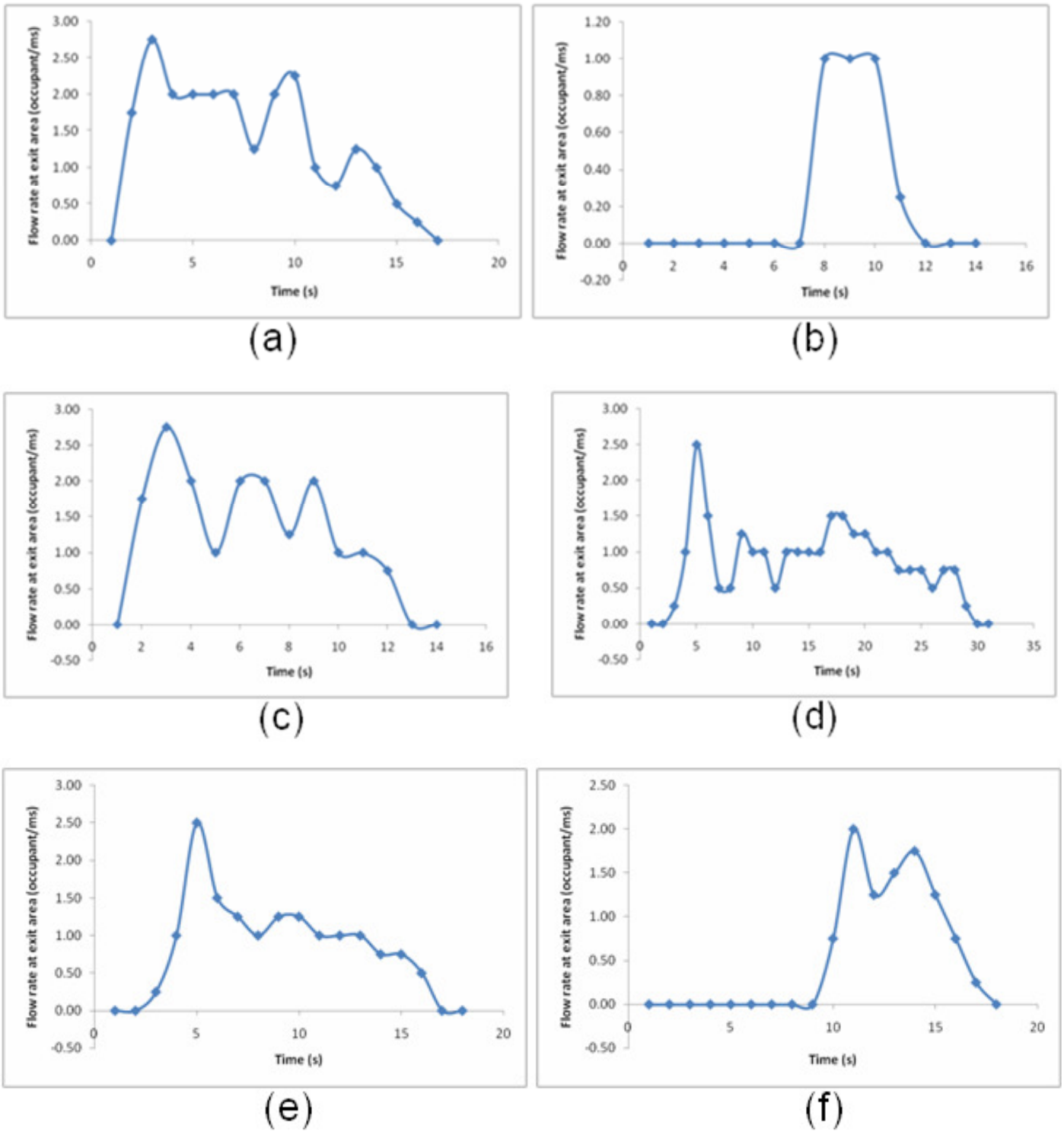

Figure 9. Plot for flow rate at exit area vs. time. Plot (a) for simulation 1, (b) and (c) for simulation 2, while (d) for simulation 3, lastly (e) and (f) are for simulation 4.

time taken by the occupants to evacuate the room. The occupants were unable to move to the nearest alternate exit because the floor-field model restricted their movement. In this floor-field model, occupants can only move to an exit according to the weight assigned to the floor where the occupant is located. This causes the occupants to tend to move to that particular nearest exit rather than switch to an alternate exit nearby.

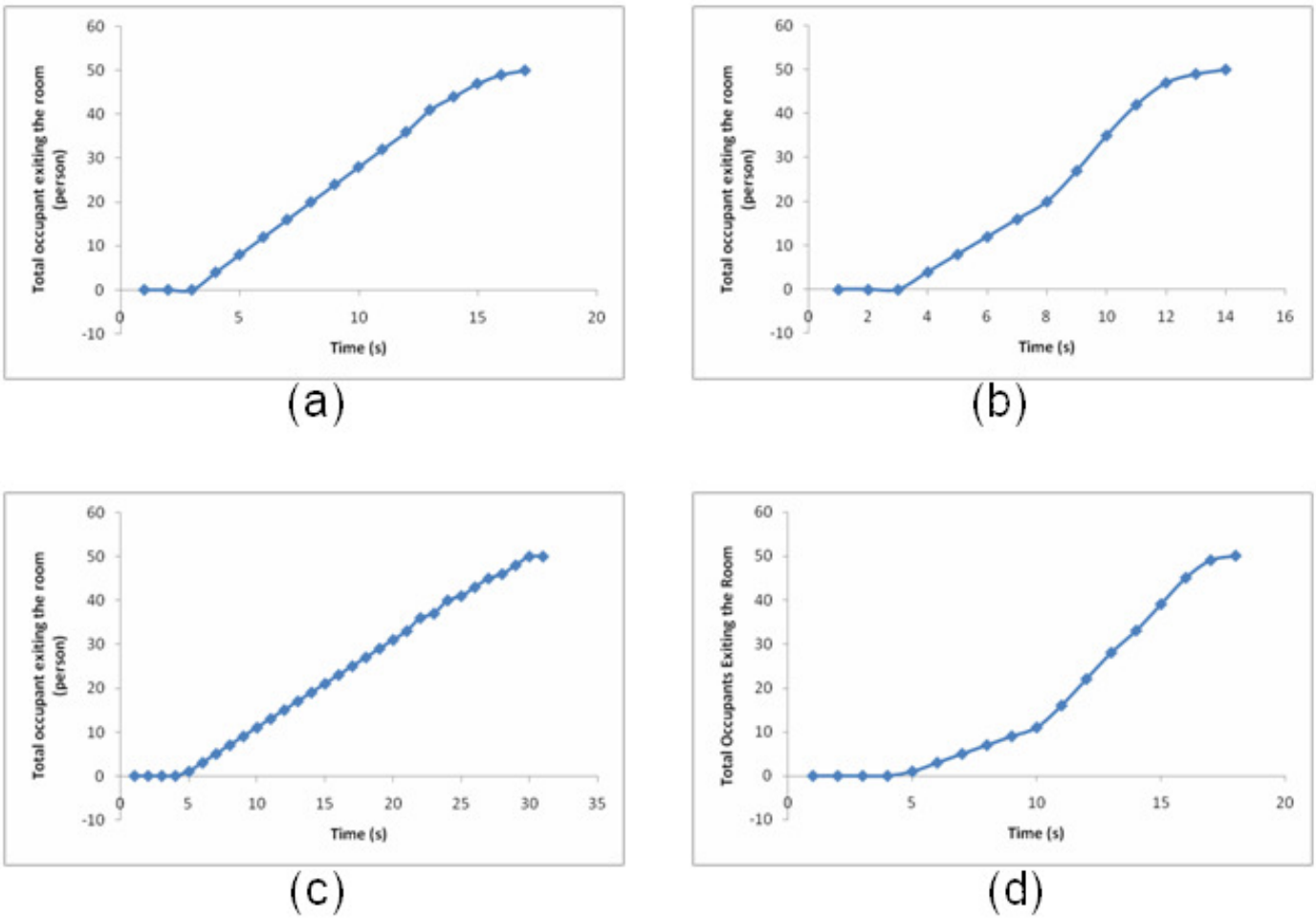

Figure 10. Plot for total occupants evacuating the room vs. time. Plot (a) for simulation 1, (b) for simulation 2, (d) for simulation 3, (e) for simulation 4.

From Figure 8(d), we can observe that the density at the exits for Simulation 3 remained at a peak for 13 s then started to decrease gradually after the total evacuation time reached 20 s. In Figure 8(e) and (f), we found that the density at the exits for Simulation 4 was distributed between two different exits. The occupants tended to move to an alternate exit when a blockage occurred near the target exit. This move of intelligent selection of exit in the proposed model reduces the peak period density about 61.54% compared to Simulation 3. Figure 8(e) and (f) show the density of Simulation 4 only at its peak for 5s at the upper exit, and at the lower exit there is no blockage. Figure 9 shows the occupant flow rate of exit against time, where the flow rate through the upper exit in both simulations was still higher than at the lower exit due to the impact of the increased density mentioned above.

Lastly, it can be seen from Figure 10(c) and (d) that the curves representing the total occupants evacuating the room differ between Simulations 3 and 4 as they gradually increase after 5 s. The difference reaches its maximum when the time reaches 15 s, and the total number of occupants evacuating the room in Simulation 4 exceeds that in Simulation 3 by about 85%.

Comparing the experiment and the simulation

Table 1 shows the data for both the simulations and the experiments. We observed that the Experiment 1 and 2 results are compatible with the Simulation 2 and 4 results respectively. The difference between Experiment 1 and Simulation 1 ranged from 25%-40%, while for Experiment 1 and Simulation 2 it ranged from 8%-15%. For the room with obstacles, the difference between Experiment 2 and Simulation 3, and Experiment 2 and Simulation 4 ranged from 51%-102% and 8%-18% respectively.

The rates of choosing the upper exit in Experiment 1 and Simulation 2 were 28% and 22% respectively, representing 14 students in Experiment 1 and 11 students in Simulation 2. Meanwhile for Experiment 2 and Simulation 4, the rates of choosing the upper exit were

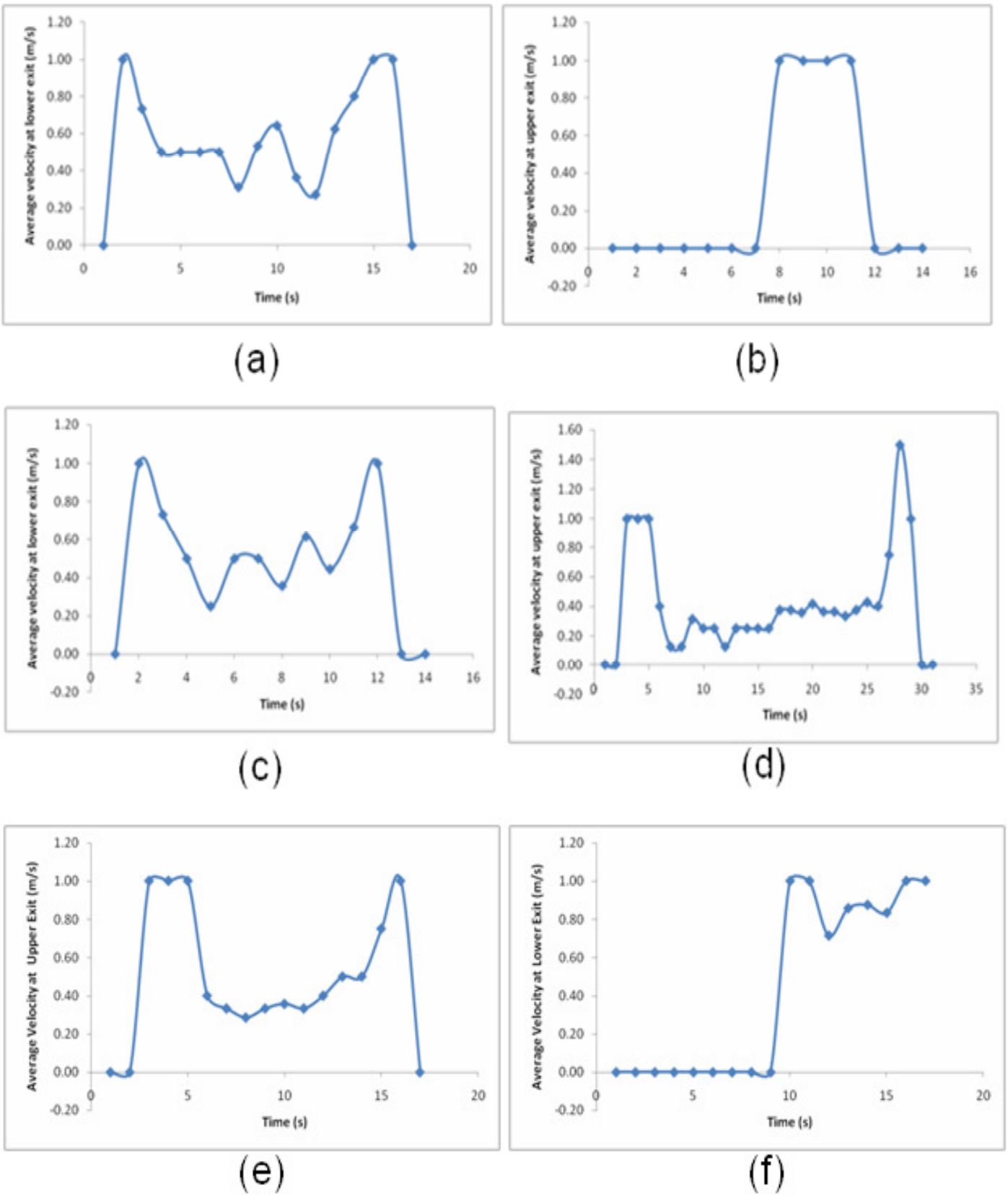

Figure 11. Plot for average velocity at exits vs. time. Plot (a) for simulation 1, (b) and (c) for simulation 2, (d) for simulation 3, (e) and (f) for simulation 4.

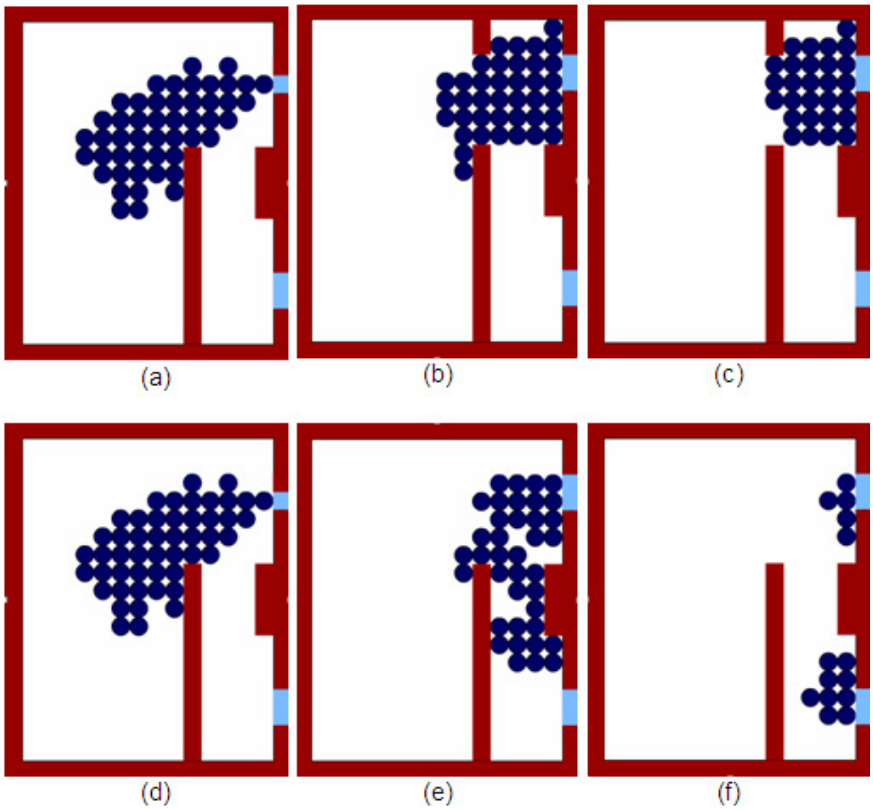

Figure 12. Snapshot for simulation. (a),(b) and (c) are snapshots from simulation 3 while (d), (e) and (f) are from simulation 4. Each represents the first 5, 10 and 15 s of the simulation.

46% and 52% respectively. On the other hand, Simulations 1 and 3 which used the floor-field model from (Varas et al., 2007) each showed a rate of choosing the upper exit of 0% and 100%. This is an extreme difference in results compared to Experiments 1 and 2.

The output flux (person) at the upper and lower exits was calculated for both the experiments and the simulations. The relationship between the flux at each exit and time are shown in Figure 13 in which the experimental data was collected every 1s. Figure 13 shows that each exit's flux curves in Experiments 1 and 2 were in sequence with the Simulation 2 and 4 results respectively. In addition, by observing Figure 13, it can be seen that people choose an exit according to two main criteria, the distance to it, and the density around it. In Experiment 1 the students preferred the lower exit which was a shorter distance from their starting location, and in Experiment 2 the students choose their first encounter exit (upper exit), located after passing by the obstacle. From both experiments, we observed that when the density at the exit increases, some students shift to an alternate exit, even though it is located further from their current position. This behavior is well reproduced in the simulation using our proposed model. Overall, the experimental and simulation results from our proposed model are reasonable and the simulation results agree with the experimental results quite well.

CONCLUSION

We carried out an evacuation experiment and simulation in a room with two exits, and then studied the evacuation process using a modified CA evacuation model incorporating neural network decision-making for intelligent exit selection. It was found that occupants prefer the closest exit to them over an alternate exit located only a little further away. In our simulation, over 2/3 of the occupants used the closest exit. The phenomena of occupants selecting an alternate exit occurred in the simulation when occupant density around that exit was high; this was observed in our proposed model.

The distribution of individual evacuation time, density around exits and the flow rate during evacuation, were compared. From our observation and study of the simulation of the exit usage with several occupants in the room, the results suggest that the exit selection behavior of occupants depends on the density around the exits.

When the density is high enough, occupants will select

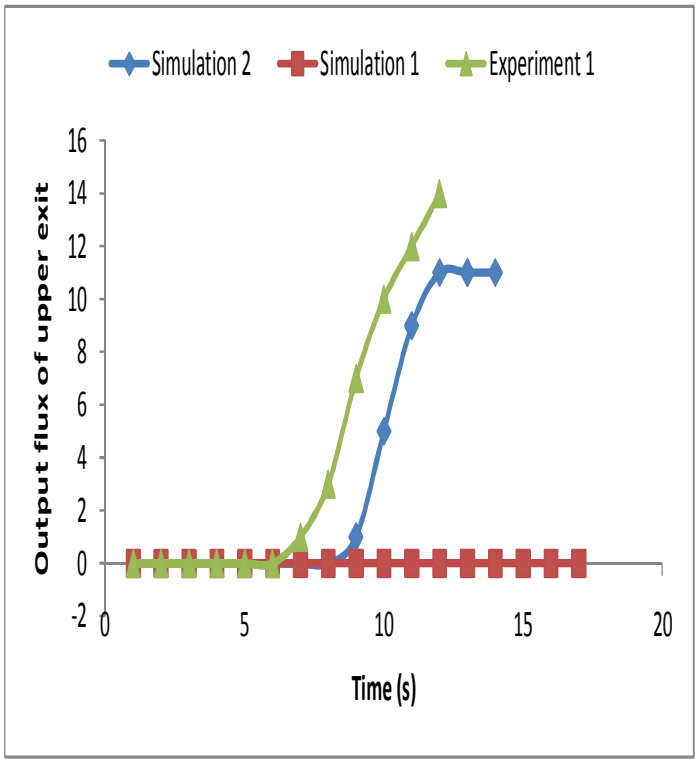

(a)

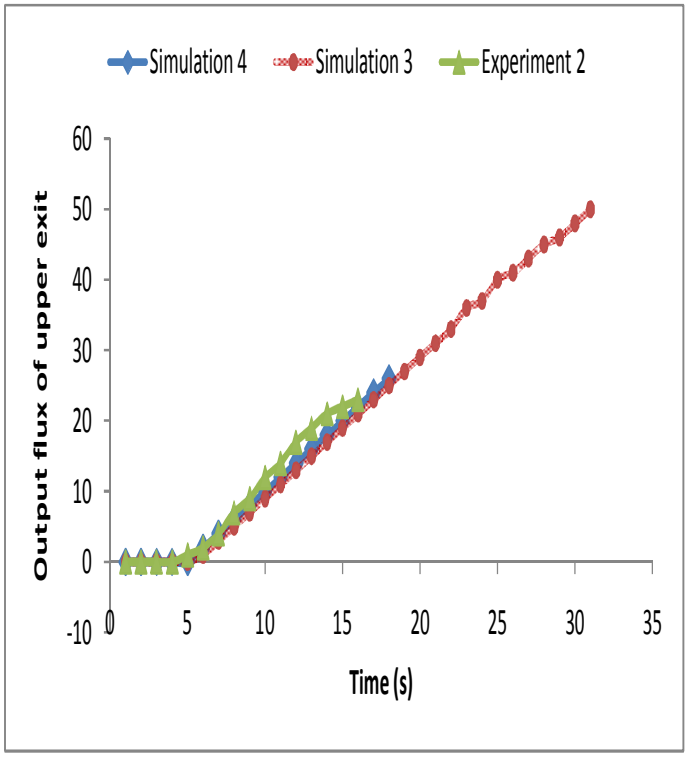

(c)

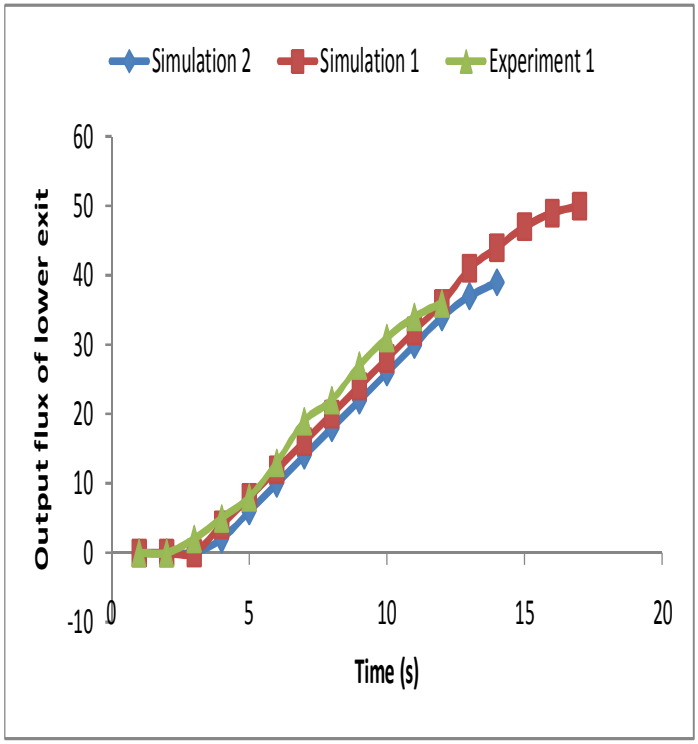

(b)

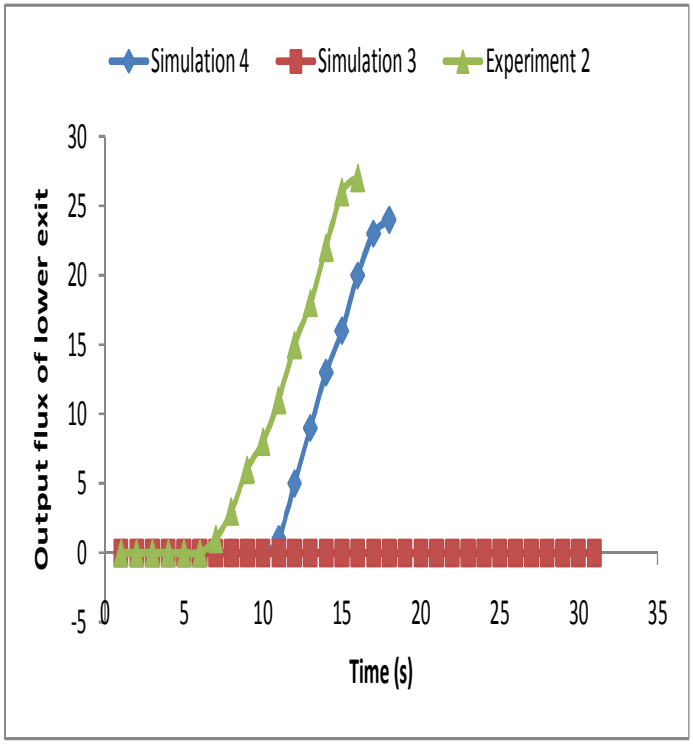

(d)

Figure 13. Plot the output flux of exit against time in experiments 1 and 2 and their simulations. (a) Output flux at upper exit for experiment 1; (b) Output flux at lower exit for experiment 1; (c) Output flux at upper exit for experiment 2; (d) Output flux at lower exit for experiment 2.

a more distant exit in order to exit more quickly. This paper reminds us that density around an exit plays an important role in an individual's deciding which exit to take; this is also stated in (Liu et al., 2009). By applying a neural network for decision-making in a CA evacuation simulation system, the evacuation model was able to simulate a more realistic outcome. Finally, from the results of this paper, it is suggested that evacuation guidance and organization should be emphasized during an emergency, since not all people will be familiar with a building's layout or will clearly know which exit is likely to be more congested during an evacuation.

REFERENCES

Alexandre D, Bastien C (2003). Cellular automata simulations of traffic: a model for city of Geneva. Networks Spatial Eco., 3: 9-21.

Burstedde C, Klauck K, Schadschneider A, Zittartz J (2001). Simulation of pedestrian dynamics using a two-dimensional cellular automaton. Physica A, 295: 507-525.

Fang ZM, Song WG, Zhang J, Wu H (2010). Experiment and modelling of exit-selecting behavior during a building evacuation. Physica A, 389: 815-824.

Helbing D, Farkas I, Viscek T (2000). Simulation of pedestrian crowds in normal and evacuation situations. Nature, 407: 487-492.

Helbing D, Farkas IJ, Vicsek T (2000). Freezing by heating in a driven mesoscopic system. Phy. Rev. Lett., 84: 1240.

Helbing D, Isobe M, Nagatani T, Takimoto K (2003). Lattice gas simulation of experimentally studied evacuation dynamics. Phy. Rev., E 67: 067101.

Helbing D, Molnar P (1995). Social force model for pedestrian dynamics. Phy. Rev., E51(5): 4282-4286.

Ishii H, Morishita S (2010). A Learning Algorithm for the Simulation of Pedestrian Flow by Cellular Automata. Cellular Automata, 6350: 465-473.

Kirchner A, Nishinari K, Schadschneider A (2003). Friction effects and clogging in a cellular automaton model for pedestrian dynamics. Phy. Rev., E65(5): 056122-056128.

Liu SB, Yang LZ, Fang TY, Li J (2009). Evacuation from a classroom considering the occupant density around exits. Physica A, 388: 1921-1928.

Mckenzie JS, Jurado JM, Pablos F (2010). Characterization of tea leaves according to their total mineral content by means of probabilistic neural networks. Food Chem., 123(3): 859-864.

Muniz AMS, Liu H, Lyons KE, Pahwa R, Liu W, Nobre FF, Nadal J (2010). Comparison among probabilistic neural network, support vector machine and logistic regression for evaluating the effect of subthalamic stimulation in Parkinson disease on ground reaction force during gait. J. Biomechanics, 43(4): 720-726.

Pablo CT, Marcela P, Marcelo LE (2007). Evacuation simulations using cellular automaton. JCS. T., 7(1): 14-20.

Peng YC, Chou CI (2011). Simulation of pedestrian flow through a "T" intersection: A multi-floor field cellular automata approach. Comp. Phy. Communication, 182: 205-208.

Song WG, Xu X, Wang BH, Ni SJ (2006). Simulation of evacuation processes using a multi-grid model for pedestrian dynamics. Physica A, 363: 492-500.

Specht DF (1990). Probabilistic neural network and the polynomial adaline as complementary techniques for classification. IEEE Trans. Neural Networks, 1(1): 111-121.

Teknomo K, Millonig A (2007). A navigation algorithm for pedestrian simulation dynamic environments. Proc. 11th World Conf. on Transport Research (WTRC): 8–16.

Varas A, Cornejo MD, Mainemer D, Toledo B, Rogan J, Munoz V, Valdivia JA (2007). Cellular automaton model for evacuation process with obstacles. Physica A, 382: 631-642.

Wang D, Kwok NM, Jia XP, Li F (2010). A Cellular Automata Based Crowd Behavior Model. Artificial Intelligence Comp. Intelligence, 6320: 218-225.

Wang Y, Li L, Huang SH (2009). Feature selection using tabu search with long-term memories and probabilistic neural networks. Pattern Recog. Lett., 30(7): 661-670.

Xu X, Song WG, Zheng HY (2008). Discretization effect in a multi-grid egress model. Physica A, 387: 5567-5574.

Yang LZ, Zhao DL, Li J, Fang TY (2005). Simulation of the kin behavior in building occupant evacuation based on Cellular Automaton. Building Env., 40: 411-415.

Zhao DL, Yang LZ, Li J (2006). Exit dynamics of occupant evacuation in an emergency. Physica A, 363: 501-511.

Zhao DL, Yang LZ, Li J (2008). Occupants' behavior of going with the crowd based on cellular automata occupant evacuation model. Physica A, 387: 3708-3719.